

## Hydromagnetic Couette flow of class-II and heat transfer through a porous medium in a rotating system with Hall effects

Gauri Shanker Seth\*, Prashanta Kumar Mandal and Rohit Sharma

*Department of Applied Mathematics, Indian School of Mines  
Dhanbad-826004, India*

*Emails: gsseth\_ism@yahoo.com, ism.prashanta@gmail.com,  
rohit.iitg08@gmail.com*

**Abstract.** Steady hydromagnetic Couette flow of class-II of a viscous, incompressible and electrically conducting fluid through a porous medium in a rotating system taking Hall current into account is investigated. Heat transfer characteristics of the fluid flow are considered taking viscous and Joule dissipations into account. It is noticed that there exists flow separation at the moving plate in the secondary flow direction on increasing either rotation parameter  $K^2$  when Hall current parameter  $m = 0.5$  or  $m$  when  $K^2 = 7$ . Also there exists flow separation at the moving plate in the secondary flow direction on increasing either magnetic parameter  $M^2$  for every value of porosity parameter  $K_1$  or  $K_1$  when  $M^2 = 15$ .

**Keywords:** Couette flow of class-II, Porous medium, Coriolis force, Hall current, viscous and Joule dissipations.

**AMS Subject Classification:** 76W05, 76U05.

### 1 Introduction

Theoretical/Experimental investigation of hydromagnetic Couette flow of a viscous, incompressible and electrically conducting fluid in a rotating sys-

\*Corresponding author.

Received: 19 September 2014 / Revised: 25 October 2014 / Accepted: 27 October 2014.

tem in the presence of an applied magnetic field has drawn attention of several researchers during past decades due to its wide range of application in natural phenomena and in a number of MHD devices viz. generators, accelerators, pumps, flow meters, nuclear reactors utilizing liquid metals etc. An order of magnitude analysis shows that, in the basic field equations, the effect of Coriolis force is more significant as compared to that of inertial and viscous forces. Furthermore, Coriolis and magnetic forces are comparable in magnitude and Coriolis force induces secondary flow in the flow-field. It is well known that the theory of Couette flow is used for the measurement of viscosity and estimating drag force in many wall driven devices. It may be noted that there exist two types of MHD Couette flows [35–37, 39] viz. (i) MHD Couette flow of class-I and (ii) MHD Couette flow of class-II. The fluid flow induced due to the movement of a plate when the fluid above the plate is bounded by stationary plate, placed at a finite distance from the moving plate, is recognized as MHD Couette flow of class-I [23, 34]. This fluid flow is similar to the flow induced by movement of a plate when the fluid at infinity i.e. fluid outside the boundary layer region (free stream) is stationary [8]. The fluid flow past a stationary plate which is induced due to movement of a plate, placed at a finite distance from the stationary plate, is identified as MHD Couette flow of class-II [35–37, 39]. This fluid flow is similar to the flow past a stationary plate due to moving free stream [8]. Mazumder [27] initiated the study of unsteady hydrodynamic Couette flow of class-II in a rotating system. Subsequently this problem is investigated by Ganapathy [18] and Das et al. [15] by considering different aspects of the problem. Seth and Singh [37, 39], Singh [40], Hayat et al. [19, 20], Seth et al. [38] and Das et al. [17] investigated MHD Couette flow of class-II in a rotating system in the presence of transverse magnetic field considering different aspects of the problem. In all these investigations, induced magnetic field produced by fluid motion is neglected in comparison to the applied magnetic field. This assumption is valid because magnetic Reynolds number is very small for liquid metals and partially ionized fluids [10]. Moreover, for the problems of geophysical and astrophysical interest and in so many MHD devices, namely, MHD energy generators, MHD pumps, plasma accelerators etc. magnetic Reynolds number is not very small so induced magnetic field cannot be neglected. Taking into consideration of this fact, Jana et al. [23] and Seth and Maiti [34] investigated steady hydromagnetic Couette flow of class-I of a viscous, incompressible and electrically conducting fluid in a rotating system under different conditions whereas Seth and Singh [36], Seth et al. [31, 32, 35] and Seth and Hussain [33] studied steady MHD Couette

flow of class-II of a viscous, incompressible and electrically conducting fluid in a rotating system taking induced magnetic field into account considering different aspects of the problem.

It is worthy to note that, in an ionized fluid whose density is low and/or applied magnetic field is strong, the effects of Hall current become significant [45]. Both Hall current and rotation induce secondary flow in the flow-field. Therefore, it seems to be important to compare and contrast the effects of these two agencies and also to study their combined effects. Hall current and rotation are likely to be important in many engineering applications viz. MHD power generators, MHD pumps and plasma flow in accelerators, geophysical and astrophysical problems of interest as well as in flows of plasmas in laboratory. Keeping in view the importance of such study, Jana and Datta [22], Seth and Ahmad [30] and Mandal et al. [26] investigated effects of Hall current on steady hydromagnetic Couette flow of class-I in a rotating system under different conditions whereas Seth et al. [31,32], Seth and Hussain [33], Sarkar et al. [29] and Das et al. [16] studied effects of Hall current and rotation on steady hydromagnetic Couette flow of class-II in a rotating system. Ahmed and Zueco [6] investigated oscillatory hydromagnetic free convection flow with heat and mass transfer in a rotating vertical porous channel taking Hall current into account.

Hydromagnetic flow through porous medium is of considerable importance because it is very much prevalent in nature and it may find applications in many biological and engineering problems such as the movement of natural gases, oil and water through the oil reservoirs, in chemical engineering for the filtration and water purification processes, to study underground water resources and seepage of water in river beds etc. Keeping in view the importance of such study, Chamkha [13] investigated non-Darcy fully developed hydromagnetic mixed convection flow through a porous medium in a channel with heat generation/absorption. In the same year Chamkha [11] also considered unsteady hydromagnetic free convection flow through a fluid saturated porous medium in a vertical channel. Alagoa et al. [7] analyzed the effects of radiation on hydromagnetic natural convection flow through a porous medium between two infinite parallel plates with time-dependent suction. Chamkha [12] discussed steady laminar flow of two viscous, incompressible, electrically conducting and heat generating/absorbing immiscible fluids in porous and non-porous channels filled with a uniform porous medium. Subsequently Chamkha [14] also investigated unsteady hydromagnetic flow and heat transfer of an electrically conducting and heat generating/absorbing fluid in a horizontal porous channel filled with uniform porous medium in the presence of electric and magnetic fields. Fluid

flow within the channel is induced due to the constant pressure gradient. Singh et al. [43] studied oscillatory Couette flow through a porous medium in rotating system. Makinde and Mhone [25] investigated the combined effects of transverse magnetic field and radiative heat transfer on unsteady flow of an optically thin radiating fluid through a channel filled with porous medium. Israel-Cookey et al. [21] presented MHD oscillatory Couette flow of a radiating viscous fluid in a porous medium with periodic wall temperature. Singh [41] analysed the effects of suction/injection on oscillatory free convection flow through a porous medium bounded by two vertical porous plates. Singh [42] obtained an exact solution of oscillatory MHD flow in a channel filled with porous medium. Prasad and Kumar [28] investigated unsteady hydromagnetic Couette flow through a porous medium in a rotating system. Jana et al. [24] discussed unsteady Couette flow of a viscous and incompressible fluid through a porous medium within porous horizontal channel in a rotating system. Singh and Mathew [44] investigated the effects of permeability and suction/injection on an oscillatory free convection flow of viscous and incompressible fluid through highly porous medium within two infinite vertical porous plates when the entire system rotates about an axis normal to the plane of the plates with uniform angular velocity  $\Omega$ . Chand et al. [9] considered oscillatory free convection flow of a viscous and incompressible fluid through porous medium in a rotating vertical channel. Ahmed and Chamkha [1] investigated Hartmann Newtonian radiating MHD flow in a rotating vertical porous channel immersed in a Darcian porous regime. The research studies on fluid flow through porous medium are also due to Umapathi et al. [46, 47], Ahmed and Kalita [2–4] and Ahmed [5].

The aim of the present investigation is to study steady hydromagnetic Couette flow of class-II and heat transfer of a viscous, incompressible and electrically conducting fluid through a uniform porous medium in the presence of a uniform transverse magnetic field taking Hall current into account. Both the fluid and channel rotate in unison with uniform angular velocity  $\Omega$  about an axis perpendicular to the plane of the plates. Fluid flow within the channel is induced due to movement of upper plate in its own plane. The moving plate of the channel is considered electrically non-conducting whereas the stationary plate is considered perfectly conducting. Exact solution of the governing equations is obtained in closed form. Expressions for the shear stress at the plates due to primary and secondary flows and mass flow rates in the primary and secondary flow directions are also derived. Asymptotic behaviour of the solution is analysed for large values of  $K^2$  and  $M^2$  to gain some physical insight into the flow pattern. Numerical values

of fluid velocity, induced magnetic field and fluid temperature, computed with the help of MATLAB software, are depicted graphically versus channel width variable  $\eta$  whereas those of shear stress and rate of heat transfer at the plates and mass flow rates are presented in tabular form for various values of pertinent flow parameters. This study may find applications in science and engineering, namely, thermonuclear engineering, geophysical and astrophysical fluid dynamics, geothermal power extraction, plasma aerodynamics, extraction of oil and gases from reservoirs, MHD power generation and manufacturing processes.

## 2 Formulation of the problem and its solution

Consider steady hydromagnetic Couette flow of class-II of a viscous, incompressible and electrically conducting fluid within two parallel plates  $z = 0$  and  $z = L$ , embedded in a uniform porous medium, in the presence of a uniform transverse magnetic field  $H_0$  which is applied in a direction parallel to  $z$ -axis. Both the fluid and channel are in a state of rigid body rotation with uniform angular velocity  $\Omega$  about  $z$ -axis. Lower plate of the channel is considered perfectly conducting whereas upper plate of the channel is assumed as electrically non-conducting. Fluid flow within the channel is induced due to the movement of the upper plate of the channel  $z = L$  with uniform velocity  $U_0$  in  $x$ -direction whereas lower plate of the channel  $z = 0$  is kept fixed. The schematic diagram of the physical problem is presented in Figure 1.

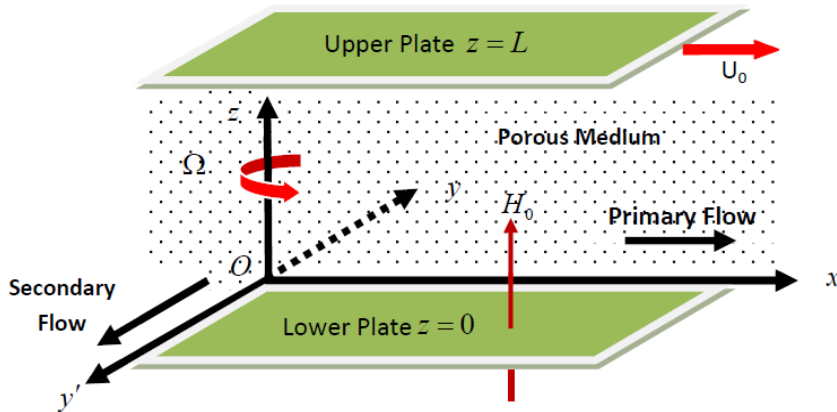


Figure 1: Schematic diagram of the physical problem

Since plates of the channel are of infinite extent in  $x$  and  $y$  directions and flow is steady, so all physical quantities, except pressure, depend on  $z$  only. Therefore, fluid velocity  $\vec{q}$  and induced magnetic field  $\vec{H}$  are assumed as

$$\vec{q} = (u_x, u_y, 0) \quad \text{and} \quad \vec{H} = (H_x', H_y', H_0), \quad (1)$$

which are in agreement with the fundamental equations of Magnetohydrodynamics in a rotating system.

Under the assumptions made above, the governing equations for the flow of a viscous, incompressible and electrically conducting fluid in a rotating system are given by

$$-2\Omega u_y = -\frac{1}{\rho} \frac{\partial p^*}{\partial x} + \nu \frac{d^2 u_x}{dz^2} + \frac{\mu_e H_0}{\rho} \frac{dH_x'}{dz} - \frac{\nu}{K'} u_x, \quad (2)$$

$$2\Omega u_x = -\frac{1}{\rho} \frac{\partial p^*}{\partial y} + \nu \frac{d^2 u_y}{dz^2} + \frac{\mu_e H_0}{\rho} \frac{dH_y'}{dz} - \frac{\nu}{K'} u_y, \quad (3)$$

$$0 = -\frac{1}{\rho} \frac{\partial p^*}{\partial z}, \quad (4)$$

$$0 = H_0 \frac{du_x}{dz} + \nu_m \frac{d^2 H_x'}{dz^2} + m\nu_m \frac{d^2 H_y'}{dz^2}, \quad (5)$$

$$0 = H_0 \frac{du_y}{dz} + \nu_m \frac{d^2 H_y'}{dz^2} - m\nu_m \frac{d^2 H_x'}{dz^2}, \quad (6)$$

where  $m = \omega_e \tau_e$  is Hall current parameter.  $u_x$ ,  $u_y$ ,  $H_x'$ ,  $H_y'$ ,  $\rho$ ,  $\nu$ ,  $\nu_m$ ,  $\mu_e$ ,  $\sigma$ ,  $K'$ ,  $p^*$ ,  $\omega_e$  and  $\tau_e$  are, respectively, fluid velocity in  $x$ -direction, fluid velocity in  $y$ -direction, induced magnetic field in  $x$ -direction, induced magnetic field in  $y$ -direction, fluid density, kinematic coefficient of viscosity, coefficient of magnetic diffusivity, magnetic permeability, electrical conductivity of the fluid, permeability of the medium, modified pressure including centrifugal force, cyclotron frequency and electron collision time. The upper plate of the channel is considered electrically non-conducting whereas lower plate of the channel is assumed as perfectly conducting. Thus the boundary conditions for the velocity and induced magnetic field are given by

$$u_x = u_y = 0; \quad \frac{dh_x}{dz} = \frac{dh_y}{dz} \quad \text{at} \quad z = 0, \quad (7a)$$

$$u_x = U_0, u_y = 0; \quad H_x' = H_y' = 0 \quad \text{at} \quad z = L. \quad (7b)$$

Equation (4) shows that modified pressure  $p^*$  is independent of  $z$ , so the values of the pressure gradient terms  $-\frac{1}{\rho} \frac{\partial p^*}{\partial x}$  and  $-\frac{1}{\rho} \frac{\partial p^*}{\partial y}$ , which are present

in the equations (2) and (3), are evaluated using boundary conditions (7b) for MHD Couette flow of class-II [35–37,39]. However, the values of pressure gradient terms  $-\frac{1}{\rho} \frac{\partial p^*}{\partial x}$  and  $-\frac{1}{\rho} \frac{\partial p^*}{\partial y}$  are zero for MHD Couette flow of class-I [23,34], which are evaluated with the help of boundary conditions (7a). Therefore, the values of pressure gradient terms for MHD Couette flow of Class-II are given by

$$-\frac{1}{\rho} \frac{\partial p^*}{\partial x} = \frac{\nu}{K'} U_0 \quad \text{and} \quad -\frac{1}{\rho} \frac{\partial p^*}{\partial y} = 2\Omega U_0. \quad (8)$$

Making use of (8), equations (2) and (3) reduce to

$$-2\Omega u_y = \nu \frac{d^2 u_x}{dz^2} + \frac{\mu_e H_0}{\rho} \frac{dH_x'}{dz} - \frac{\nu}{K'} (u_x - U_0), \quad (9)$$

$$2\Omega (u_x - U_0) = \nu \frac{d^2 u_y}{dz^2} + \frac{\mu_e H_0}{\rho} \frac{dH_y'}{dz} - \frac{\nu}{K'} u_y. \quad (10)$$

To present equations (5), (6), (9) and (10) along with the boundary conditions (7a) and (7b) in non-dimensional form, the following non-dimensional variables are introduced.

$$\eta = \frac{z}{L}, u = \frac{u_x}{U_0}, v = \frac{u_y}{U_0}, H_x = \frac{H_x'}{H_0}, H_y = \frac{H_y'}{H_0}. \quad (11)$$

Equations (5), (6), (9) and (10) with the use of (11) assume the following form

$$-2K^2 v = \frac{d^2 u}{d\eta^2} + \frac{M^2}{R_m} \frac{dH_x}{d\eta} - \frac{1}{K_1} (u - 1), \quad (12)$$

$$2K^2 (u - 1) = \frac{d^2 v}{d\eta^2} + \frac{M^2}{R_m} \frac{dH_y}{d\eta} - \frac{1}{K_1} v, \quad (13)$$

$$0 = \frac{du}{d\eta} + \frac{1}{R_m} \frac{d^2 H_x}{d\eta^2} + \frac{m}{R_m} \frac{d^2 H_y}{d\eta^2}, \quad (14)$$

$$0 = \frac{dv}{d\eta} + \frac{1}{R_m} \frac{d^2 H_y}{d\eta^2} - \frac{m}{R_m} \frac{d^2 H_x}{d\eta^2}, \quad (15)$$

where  $K^2 = \frac{\Omega L^2}{\nu}$  is rotation parameter (reciprocal of Ekman number),  $M^2 = \frac{\mu_e H_0^2 L^2}{\rho \nu \nu_m}$  is magnetic parameter (square of Hartmann number),  $R_m = \frac{U_0 L}{\nu_m}$  is magnetic Reynolds number and  $K_1 = \frac{K'}{L^2}$  is porosity parameter. Boundary conditions (7a) and (7b), in non-dimensional form, become

$$u = v = 0; \quad \frac{dH_x}{d\eta} = \frac{dH_y}{d\eta} = 0 \quad \text{at} \quad \eta = 0, \quad (16a)$$

$$u = 1, v = 0; \quad H_x = H_y = 0 \quad \text{at} \quad \eta = 1. \quad (16b)$$

Equations (12) to (15) are presented in compact form which are given by

$$2iK^2 f = \frac{d^2 f}{d\eta^2} + M^2 \frac{db}{d\eta} - \frac{f}{K_1}, \quad (17)$$

$$0 = \frac{df}{d\eta} + \frac{d^2 b}{d\eta^2} - mi \frac{d^2 b}{d\eta^2}, \quad (18)$$

where

$$f = u + iv - 1, \quad b = h_x + ih_y, \quad h_x = \frac{H_x}{R_m} \text{ and } h_y = \frac{H_y}{R_m}.$$

Boundary conditions (16a) and (16b), in compact form, are

$$f = -1; \quad \frac{db}{d\eta} = 0 \quad \text{at} \quad \eta = 0, \quad (19a)$$

$$f = 0; \quad b = 0 \quad \text{at} \quad \eta = 1. \quad (19b)$$

Equations (17) and (18) subject to the boundary conditions (19a) and (19b) are solved and the solution for fluid velocity and induced magnetic field are expressed in the following form

$$F(\eta) = -(1 - im) [A \{\cosh \lambda\eta - 1\} + B \sinh \lambda\eta], \quad (20)$$

$$b(\eta) = \frac{1}{\lambda} [A \{\sinh \lambda\eta - \sinh \lambda\} + B \{\cosh \lambda\eta - \cosh \lambda\}] + A(1 - \eta), \quad (21)$$

where

$$F(\eta) = u + iv, \quad \lambda = \alpha + i\beta,$$

$$\alpha, \beta = \frac{1}{\sqrt{2}} \left[ \left\{ \left( \frac{M^2}{1+m^2} + \frac{1}{K_1} \right)^2 + \left( 2K^2 + \frac{M^2 m}{1+m^2} \right)^2 \right\}^{\frac{1}{2}} \pm \left( \frac{M^2}{1+m^2} + \frac{1}{K_1} \right) \right]^{\frac{1}{2}},$$

$$A = \frac{1}{\lambda^2} \left[ \frac{(2iK_1K^2+1)(1+im)}{K_1(1+m^2)} \right]$$

$$B = \frac{1}{\lambda^2} \left[ \frac{\{(2iK_1K^2+1)(1-\cosh \lambda) - \lambda^2 K_1\}(1+im)}{K_1(1+m^2) \sinh \lambda} \right].$$

## 2.1 Non-dimensional shear stress at the plates

Non-dimensional shear stress components  $\tau_x$  and  $\tau_y$  due to primary and secondary flows at the stationary and moving plates of the channel are given by

$$\tau_x + i\tau_y |_{\eta=0} = -(1 - im) \lambda B, \quad (22)$$

$$\tau_x + i\tau_y |_{\eta=1} = -(1 - im) \lambda [A \sinh \lambda + B \cosh \lambda]. \quad (23)$$

where  $\tau_x|_{\eta=0}$  and  $\tau_x|_{\eta=1}$  are non-dimensional shear stress at the stationary and moving plates of the channel respectively due to primary flow.  $\tau_y|_{\eta=0}$  and  $\tau_y|_{\eta=1}$  are non-dimensional shear stress at the stationary and moving plates of the channel respectively due to secondary flow.

## 2.2 Non-dimensional mass flow rates

Non-dimensional mass flow rates  $Q_x$  and  $Q_y$  in the primary and secondary flow directions respectively are given by

$$Q_x + iQ_y = - (1 - im) \left[ \frac{1}{\lambda} \{ A (\sinh \lambda - \lambda) + B (\cosh \lambda - 1) \} \right]. \quad (24)$$

## 3 Asymptotic behaviour of the solution

We shall now analyse the asymptotic behaviour of the solutions prescribed by (20) and (21) for large values of  $K^2$  and  $M^2$  to gain some physical insight into the flow pattern.

**Case I:** When  $K^2 \gg 1$  and  $M^2 \sim O(1)$ .

In this case, fluid flow becomes boundary layer type. For the boundary layer flow near the stationary plate  $\eta = 0$ , the expressions of fluid velocity and induced magnetic field, given by (20) and (21), assume the following form

$$u = 1 - e^{-\alpha_1 \eta} \cos(\beta_1 \eta) + \frac{M^2}{2K^2(1+m^2)} [m \{ e^{-\alpha_1 \eta} \cos(\beta_1 \eta) - 1 \} - e^{-\alpha_1 \eta} \sin(\beta_1 \eta)], \quad (25)$$

$$v = e^{-\alpha_1 \eta} \sin(\beta_1 \eta) - \frac{M^2}{2K^2(1+m^2)} [\{ e^{-\alpha_1 \eta} \cos(\beta_1 \eta) - 1 \} + m e^{-\alpha_1 \eta} \sin(\beta_1 \eta)], \quad (26)$$

$$h_x = \frac{1}{1+m^2} \left[ \left\{ 1 - \frac{M^2 m}{K^2(1+m^2)} \right\} \left\{ (1-\eta) - \frac{e^{-\alpha_1 \eta}}{\alpha_1^2 + \beta_1^2} (\alpha_1 \cos(\beta_1 \eta) - \beta_1 \sin(\beta_1 \eta)) \right\} - \left\{ m - \frac{M^2 (m^2 - 1)}{2K^2(1+m^2)} \right\} \frac{e^{-\alpha_1 \eta}}{\alpha_1^2 + \beta_1^2} \times (\alpha_1 \sin(\beta_1 \eta) + \beta_1 \cos(\beta_1 \eta)) \right], \quad (27)$$

$$\begin{aligned}
h_y = & \frac{1}{1+m^2} \left[ \left\{ m - \frac{M^2(m^2-1)}{2K^2(1+m^2)} \right\} \left\{ (1-\eta) - \frac{e^{-\alpha_1\eta}}{\alpha_1^2 + \beta_1^2} (\alpha_1 \cos(\beta_1\eta) \right. \right. \\
& \left. \left. - \beta_1 \sin(\beta_1\eta)) \right\} + \left\{ 1 - \frac{M^2m}{K^2(1+m^2)} \right\} \frac{e^{-\alpha_1\eta}}{\alpha_1^2 + \beta_1^2} \times \right. \\
& \left. (\alpha_1 \sin(\beta_1\eta) + \beta_1 \cos(\beta_1\eta)) \right], \tag{28}
\end{aligned}$$

where

$$\alpha_1, \beta_1 = K \left[ 1 \pm \frac{1}{4K_1 K^2} \pm \frac{M^2(1 \pm m)}{4(1+m^2)K^2} \right]. \tag{29}$$

It is evident from the expressions (25) to (28) that there arises a thin boundary layer of thickness  $O(\alpha_1^{-1})$  near stationary plate of the channel. This boundary layer may be identified as modified Ekman boundary layer and can be viewed as classical Ekman boundary layer modified by Hall current, magnetic field and permeability of the medium. The numerical values for the thickness of the boundary layer are calculated for various values of  $m$  and  $K_1$ , and are presented in Table 1.

Table 1: Thickness of the boundary layer near the stationary plate of channel when  $K^2 = 7$  and  $M^2 = 10$ .

$K_1 \downarrow m \rightarrow$	$\frac{1}{\alpha_1}$			$\frac{1}{\alpha_2}$		
	0.5	1	1.5	0.5	1	1.5
0.2	0.2352	0.2461	0.2601	0.2346	0.2308	0.2265
0.4	0.2490	0.2613	0.2771	0.2594	0.2565	0.2534
0.6	0.2540	0.2668	0.2833	0.2688	0.2664	0.2638

Expressions in (29) and Table 1 reveal that an increase in  $K^2$  and  $M^2$  leads to a decrease in  $\frac{1}{\alpha_1}$  whereas an increase in  $m$  and  $K_1$  leads to an increase in  $\frac{1}{\alpha_1}$ . This implies that rotation and magnetic field tend to reduce the thickness of the boundary layer whereas Hall current and permeability of the medium tend to enhance the thickness of the boundary layer. Similar type of boundary layer arises near the moving plate of the channel. The exponential terms in the expressions (25) to (28) damp out quickly as  $\eta$  increases.

When  $\eta \geq \frac{1}{\alpha_1}$  i.e. outside the boundary layer region, expressions (25) to (28) assume the following form

$$u \approx 1 - \frac{mM^2}{2K^2(1+m^2)}, \quad v \approx \frac{M^2}{2K^2(1+m^2)}, \tag{30}$$

$$h_x \approx \frac{(1-\eta)}{1+m^2} \left\{ 1 - \frac{M^2 m}{K^2(1+m^2)} \right\}, h_y \approx \frac{(1-\eta)}{1+m^2} \left\{ m - \frac{M^2(m^2-1)}{2K^2(1+m^2)} \right\} \quad (31)$$

Expressions in (30) and (31) reveal that, in the central core region, i.e. outside the boundary layer region, fluid flows in both the primary and secondary flow directions. Primary as well as secondary fluid velocity is affected by Hall current, magnetic field and rotation. Also induced magnetic field persist in both the primary and secondary flow directions and vary linearly with  $\eta$ . Both the primary and secondary induced magnetic fields have considerable effects of Hall current, magnetic field and rotation.

**Case II:** When  $M^2 \gg 1$  and  $K^2 \sim O(1)$ .

In this case also boundary layer type flow is expected. For the boundary layer flow near the stationary plate  $\eta = 0$ , the expressions of fluid velocity and induced magnetic field, presented by (20) and (21), reduce to

$$u = \frac{1}{M^2} \left[ \left( \frac{1}{K_1} + 2K^2 m \right) \{1 - e^{-\alpha_2 \eta} \cos(\beta_2 \eta)\} + \left( \frac{m}{K_1} - 2K^2 \right) \times e^{-\alpha_2 \eta} \sin(\beta_2 \eta) \right], \quad (32)$$

$$v = \frac{1}{M^2} \left[ \left( 2K^2 - \frac{m}{K_1} \right) \{1 - e^{-\alpha_2 \eta} \cos(\beta_2 \eta)\} + \left( \frac{1}{K_1} + 2K^2 m \right) \times e^{-\alpha_2 \eta} \sin(\beta_2 \eta) \right], \quad (33)$$

$$h_x = \frac{1}{K_1 M^2} \left[ (1-\eta) - \frac{e^{-\alpha_2 \eta}}{\alpha_2^2 + \beta_2^2} \{ \alpha_2 \cos(\beta_2 \eta) - \beta_2 \sin(\beta_2 \eta) \} \right] - \frac{2K^2}{M^2} \left[ \frac{e^{-\alpha_2 \eta}}{\alpha_2^2 + \beta_2^2} \{ \alpha_2 \sin(\beta_2 \eta) + \beta_2 \cos(\beta_2 \eta) \} \right], \quad (34)$$

$$h_y = \frac{2K^2}{M^2} \left[ (1-\eta) - \frac{e^{-\alpha_2 \eta}}{\alpha_2^2 + \beta_2^2} \{ \alpha_2 \cos(\beta_2 \eta) - \beta_2 \sin(\beta_2 \eta) \} \right] + \frac{1}{K_1 M^2} \left[ \frac{e^{-\alpha_2 \eta}}{\alpha_2^2 + \beta_2^2} \{ \alpha_2 \sin(\beta_2 \eta) + \beta_2 \cos(\beta_2 \eta) \} \right], \quad (35)$$

where

$$\alpha_2 = \frac{M}{1+m^2} (\alpha^* + m\beta^*) + \frac{1}{2K_1 M} \alpha^* + \frac{K^2}{M} \beta^*, \quad (36)$$

$$\beta_2 = \frac{M}{1+m^2} (m\alpha^* - \beta^*) + \frac{K^2}{M} \alpha^* - \frac{1}{2K_1 M} \beta^*,$$

$$\alpha^* = \frac{1}{\sqrt{2}} \{(1 + m^2)^{\frac{1}{2}} + 1\}^{\frac{1}{2}},$$

$$\beta^* = \frac{1}{\sqrt{2}} \{(1 + m^2)^{\frac{1}{2}} - 1\}^{\frac{1}{2}}.$$

It is evident from the expressions (32) to (35) that there arises a thin boundary layer of thickness  $O(\alpha_2^{-1})$  near stationary plate of the channel. This boundary layer may be identified as modified Hartmann boundary layer and can be viewed as classical Hartman boundary layer modified by Hall current, rotation and permeability of the medium. The numerical values for the thickness of the boundary layer are calculated for various values of  $m$  and  $K_1$ , and are displayed in Table 1.

Expressions in (36) and Table 1 reveal that an increase in  $m$ ,  $K^2$  and  $M^2$  leads to a decrease in  $\frac{1}{\alpha_2}$  whereas an increase in  $K_1$  leads to an increase in  $\frac{1}{\alpha_2}$ . This implies that Hall current, rotation and magnetic field tend to reduce the thickness of the boundary layer whereas permeability of the medium tends to enhance the thickness of the boundary layer. Similar type of boundary layer arises near the moving plate of the channel.

In the central core region, expressions (32) to (35) take the following form

$$u \approx \frac{1}{M^2} \left( \frac{1}{K_1} + 2K^2 m \right), \quad v \approx \frac{1}{M^2} \left( 2K^2 - \frac{m}{K_1} \right), \quad (37)$$

$$h_x \approx \frac{1}{K_1 M^2} (1 - \eta), \quad h_y \approx \frac{2K^2}{M^2} (1 - \eta). \quad (38)$$

Expressions in (37) and (38) reveal that, in the central core region, fluid flows in both the primary and secondary flow directions and both the primary and secondary velocities are affected by Hall current, magnetic field, rotation and permeability of the medium. Also both the primary and secondary induced magnetic fields persist in the central core region. Primary induced magnetic field is unaffected by rotation and Hall current whereas secondary induced magnetic field is unaffected by permeability of the medium and Hall current. Also both the induced magnetic field have considerable effects of magnetic field and vary linearly with  $\eta$ .

## 4 Heat transfer characteristics

We shall now discuss heat transfer characteristics of the fluid flow. The stationary and moving plates of the channel are maintained at uniform temperature  $T_0$  and  $T_1$  respectively, where  $T_0 < T < T_1$ ,  $T$  being the fluid

temperature.

Energy equation, taking viscous and Joule dissipations into account, is given by

$$\begin{aligned} \alpha^* \frac{d^2 T}{dz^2} + \frac{\nu}{C_p} \left[ \left( \frac{du_x}{dz} \right)^2 + \left( \frac{du_y}{dz} \right)^2 \right] + \frac{\nu}{K' C_p} [(u_x - U_0)^2 + u_y^2] \\ + \frac{1}{\sigma \rho C_p} \left[ \left( \frac{dH_x'}{dz} \right)^2 + \left( \frac{dH_y'}{dz} \right)^2 \right] = 0, \end{aligned} \quad (39)$$

where  $\alpha^*$  and  $C_p$  are thermal diffusivity of fluid and specific heat at constant pressure respectively.

Boundary conditions for the fluid temperature are

$$T = T_0 \quad \text{at} \quad z = 0; \quad T = T_1 \quad \text{at} \quad z = L. \quad (40)$$

Equation (39), in non-dimensional form, becomes

$$\begin{aligned} \frac{d^2 \theta}{d\eta^2} + P_r E_c \left[ \left\{ \left( \frac{du}{d\eta} \right)^2 + \left( \frac{dv}{d\eta} \right)^2 \right\} + \frac{1}{K_1} \left\{ (u - 1)^2 + v^2 \right\} \right. \\ \left. + M^2 \left\{ \left( \frac{dh_x}{d\eta} \right)^2 + \left( \frac{dh_y}{d\eta} \right)^2 \right\} \right] = 0, \end{aligned} \quad (41)$$

where  $\theta = \frac{T - T_0}{T_1 - T_0}$ ,  $P_r = \frac{\nu}{\alpha^*}$  and  $E_c = \frac{U_0^2}{C_p(T_1 - T_0)}$  are non-dimensional fluid temperature, Prandtl number and Eckert number respectively.

Boundary conditions (40), in non-dimensional form, become

$$\theta = 0 \quad \text{at} \quad \eta = 0; \quad \theta = 1 \quad \text{at} \quad \eta = 1. \quad (42)$$

Using analytical solutions for the fluid velocity and induced magnetic field given by (20) and (21) in equation (41), the resulting differential equation subject to the boundary conditions (42) is solved numerically using MATLAB software. The numerical values of rate of heat transfer at the stationary and moving plates of the channel are also computed with the help of MATLAB software.

## 5 Validation of results

In order to establish the accuracy of our results, we have compared our results in case of non-porous medium with those of Sarkar et al. [29]. Both the results are displayed graphically in Figure 2. It is evident from Figure 2 that our results are in excellent agreement with the results of Sarkar et al. [29].

## 6 Results and discussion

In order to study the effects of Hall current, magnetic field, rotation and permeability of the medium on the flow-field, the numerical values of fluid velocity and induced magnetic field, computed from the analytical solution given by (20) and (21), are displayed graphically versus channel width variable  $\eta$  in Figures 2 to 9 for various values of Hall current parameter  $m$ , rotation parameter  $K^2$ , magnetic parameter  $M^2$  and porosity parameter  $K_1$ . All parametric values corresponding to each figure are included therein. It should be noted that  $M^2 = 10, 15$  and  $20$  imply the presence of strong magnetic field. Figure 2 illustrates the influence of rotation on both the primary and secondary fluid velocities  $u$  and  $v$  respectively. It is noticed from Figure 2 that  $u$  as well as  $v$  increases on increasing  $K^2$ . This implies that rotation tends to accelerate fluid flow in both the primary and secondary flow directions. Figure 3 manifests the effect of Hall current on both the primary and secondary fluid velocities. It is evident from Figure 3 that  $u$  increases whereas  $v$  decreases on increasing  $m$ . This implies that Hall current tends to accelerate fluid flow in the primary flow direction whereas it has a reverse effect on the fluid flow in the secondary flow direction. Figure 4 demonstrates the effect of magnetic field on both the primary and secondary fluid velocities. Figure 4 reveals that both  $u$  and  $v$  decrease on increasing  $M^2$ . This implies that magnetic field tends to decelerate fluid flow in both the primary and secondary flow directions. Figure 5 manifests the effect of permeability of the medium on both the primary and secondary fluid velocities. It is evident from Figure 5 that  $u$  decreases whereas  $v$  increases on increasing  $K_1$ . This implies that permeability of the medium tends to decelerate the fluid flow in the primary flow direction whereas it has a reverse effect on the fluid flow in the secondary flow direction. Figure 6 depicts the effect of Hall current on both the primary and secondary induced magnetic fields  $h_x$  and  $h_y$  respectively. It is evident from Figure 6 that  $h_x$  decreases whereas  $h_y$  behaves in oscillatory manner on increasing  $m$ . This implies that Hall current tends to reduce primary induced magnetic field. Figure 7 depicts the influence of rotation on both the primary and secondary induced magnetic fields. It is revealed from Figure 7 that both  $h_x$  and  $h_y$  increase on increasing  $K^2$ . This implies that rotation tends to enhance both the primary and secondary induced magnetic fields. Figure 8 depicts the influence of magnetic field on both the primary and secondary induced magnetic fields. It is revealed from Figure 8 that both  $h_x$  and  $h_y$  decrease on increasing  $M^2$ . This implies that magnetic field tends to reduce both the primary and secondary induced magnetic fields. Figure 9 displays the influence of permeability of the medium on both the

primary and secondary induced magnetic fields. It is noticed from Figure 9 that  $h_x$  decreases whereas  $h_y$  increases on increasing  $K_1$ . This implies that permeability of the medium tends to reduce the primary induced magnetic field whereas it has a reverse effect on the secondary induced magnetic field.

The numerical solution of the energy equation (41), computed using MATLAB software, is displayed graphically versus channel width variable  $\eta$  in Figures 10 to 13 for various values of  $m$ ,  $K^2$ ,  $M^2$  and  $K_1$  taking Prandtl number  $P_r = 7$  and Eckert number  $E_c = 0.2$ . All parametric values corresponding to each figure are included therein. Figure 10 displays the influence of Hall current on the fluid temperature  $\theta$ . It is evident from Figure 10 that, with an increase in  $m$ ,  $\theta$  increases in the region  $0 \leq \eta < 0.2$  whereas it decreases in the region  $0.2 \leq \eta \leq 1$ . This implies that Hall current tends to enhance fluid temperature in the region near the stationary plate whereas it has a reverse effect on the fluid temperature in most of the region of the channel. Figure 11 shows the effect of rotation on the fluid temperature  $\theta$ . It is evident from Figure 11 that, with an increase in  $K^2$ ,  $\theta$  increases in the region  $0 \leq \eta < 0.8$  whereas it decreases in the region  $0.8 \leq \eta \leq 1$ . This implies that rotation tends to enhance fluid temperature in most of the region of the channel whereas it has a reverse effect on the fluid temperature in the region near the moving plate of the channel. Figure 12 depicts the effect of magnetic field on the fluid temperature  $\theta$ . It is noticed from Figure 12 that, with an increase in  $M^2$ ,  $\theta$  decreases in the region  $0 \leq \eta < 0.2$  whereas it increases in the region  $0.2 \leq \eta \leq 1$ . This implies that magnetic field tends to reduce fluid temperature in the region near the stationary plate of the channel whereas it tends to enhance fluid temperature in most of the region of the channel. Figure 13 reveals the effect of permeability of the medium on the fluid temperature  $\theta$ . It is evident from Figure 13 that  $\theta$  decreases on increasing  $K_1$ . This implies that permeability of the medium tends to reduce fluid temperature throughout the channel.

The numerical values of primary shear stress  $\tau_x$  and secondary shear stress  $\tau_y$  at the stationary and moving plates of the channel and those of primary and secondary mass flow rates  $Q_x$  and  $Q_y$ , calculated from the analytical expressions (22) to (24), are displayed in tabular form in Tables 2 to 7 for various values of  $m$ ,  $K^2$ ,  $M^2$  and  $K_1$ . All parametric values corresponding to each table are included therein. Negative values of shear stress imply that frictional force acts in opposite direction. It is found from Tables 2 and 3 that primary shear stress at the stationary plate i.e.  $\tau_x |_{\eta=0}$  increases whereas secondary shear stress at the stationary plate i.e.  $\tau_y |_{\eta=0}$  decreases on increasing  $m$ . Both  $\tau_x |_{\eta=0}$  and  $\tau_y |_{\eta=0}$  increase

on increasing  $K^2$  whereas it decrease on increasing  $M^2$ .  $\tau_x|_{\eta=0}$  decreases whereas  $\tau_y|_{\eta=0}$  increases on increasing  $K_1$ . This implies that Hall current tends to enhance the primary shear stress at the stationary plate whereas it has a reverse effect on the secondary shear stress at the stationary plate. Rotation has a tendency to enhance both the primary and secondary shear stress at the stationary plate whereas magnetic field has a reverse effect on both the primary and secondary shear stress at the stationary plate. Permeability of the medium tends to reduce primary shear stress at the stationary plate whereas it has a reverse effect on the secondary shear stress at the stationary plate. Tables 4 and 5 reveal that primary shear stress at the moving plate i.e.  $\tau_x|_{\eta=1}$  decreases on increasing either  $m$  or  $K^2$  whereas it increases on increasing either  $M^2$  or  $K_1$ . Secondary shear stress at the moving plate i.e.  $\tau_y|_{\eta=1}$  increases on increasing  $m$  whereas it decreases on increasing  $K^2$  when  $m \geq 1$ .  $\tau_y|_{\eta=1}$  decreases in magnitude, attains a minimum, and then increases on increasing  $M^2$  whereas it increases in magnitude on increasing  $K_1$  when  $M^2 = 10$  and decreases on increasing  $K_1$  when  $M^2 = 20$ . This implies that Hall current and rotation tend to reduce primary shear stress at the moving plate whereas magnetic field and permeability of the medium have reverse effect on it. Hall current tends to enhance secondary shear stress at the moving plate whereas rotation has a reverse effect on it when  $m \geq 1$ . Permeability of the medium tends to enhance secondary shear stress at the moving plate when  $M^2 = 10$  and has a reverse effect on it when  $M^2 = 20$ . It is interesting to note from Tables 4 and 5 that there exists flow separation at the moving plate in the secondary flow direction on increasing either  $K^2$  when  $m = 0.5$  or  $m$  when  $K^2 = 7$ . Also there exists flow separation at the moving plate in the secondary flow direction on increasing either  $M^2$  for every value of  $K_1$  or  $K_1$  when  $M^2 = 15$ . It is found from Tables 6 and 7 that primary mass flow rate  $Q_x$  increases on increasing either  $m$  or  $K^2$  whereas it decreases on increasing either  $M^2$  or  $K_1$ . Secondary mass flow rate  $Q_y$  decreases on increasing either  $m$  or  $M^2$  whereas it increases on increasing either  $K^2$  or  $K_1$ . This implies that Hall current and rotation tend to enhance primary mass flow rate whereas magnetic field and permeability of medium have reverse effect on it. Rotation and permeability of the medium tend to enhance secondary mass flow rate whereas Hall current and magnetic field have reverse effect on it.

The numerical values of rate of heat transfer at the stationary as well as moving plate are computed with the help of MATLAB software and are displayed in tabular form in Tables 8 to 10 for various values of  $m$ ,  $K^2$ ,  $M^2$ ,  $K_1$ ,  $P_r$  and  $E_c$ . All parametric values corresponding to each table are

included therein. Negative values of rate of heat transfer at the moving plate imply that, there is a transfer of heat from fluid to the plate due to viscous and Joule dissipations. It is noticed from Tables 8 and 9 that rate of heat transfer at the stationary plate i.e.  $\frac{d\theta}{d\eta} |_{\eta=0}$  increases on increasing either  $m$  or  $K^2$  whereas it decreases on increasing either  $M^2$  or  $K_1$ . Rate of heat transfer at the moving plate i.e.  $\frac{d\theta}{d\eta} |_{\eta=1}$  decreases on increasing either  $m$  or  $K^2$  whereas it increases on increasing either  $M^2$  or  $K_1$ . This implies that Hall current and rotation tend to enhance rate of heat transfer at the stationary plate whereas these agencies have reverse effect on rate of heat transfer at the moving plate. Magnetic field and permeability of the medium tend to reduce rate of heat transfer at the stationary plate whereas these agencies have reverse effect on rate of heat transfer at the moving plate. It is evident from Table 10 that  $\frac{d\theta}{d\eta} |_{\eta=0}$  and  $\frac{d\theta}{d\eta} |_{\eta=1}$  increase on increasing either  $P_r$  or  $E_c$ . Since  $P_r$  measures relative strength of viscosity to thermal diffusivity,  $P_r$  decreases on increasing thermal diffusivity of medium. This implies that thermal diffusion tends to reduce rate of heat transfer at both the plates whereas viscous dissipation has a reverse effect on it.

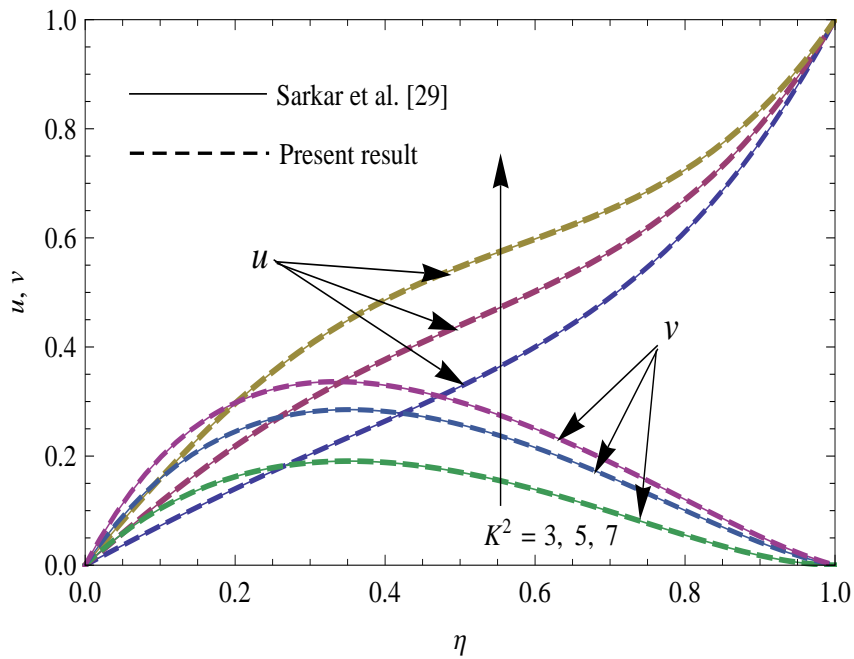


Figure 2: Velocity profiles when  $m = 0.5$ ,  $M^2 = 10$  and  $K_1 \rightarrow \infty$ .

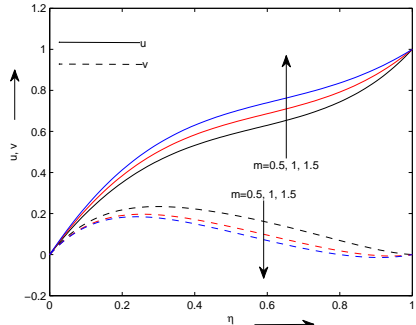


Figure 3: Velocity profiles when  $K^2 = 7$ ,  $M^2 = 10$  and  $K_1 = 0.2$ .

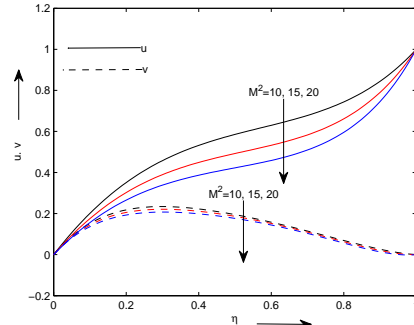


Figure 4: Velocity profiles when  $m = 0.5$ ,  $K^2 = 7$  and  $K_1 = 0.2$ .

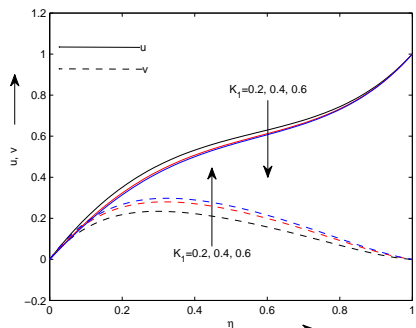


Figure 5: Velocity profiles when  $m = 0.5$ ,  $K^2 = 7$  and  $M^2 = 10$ .

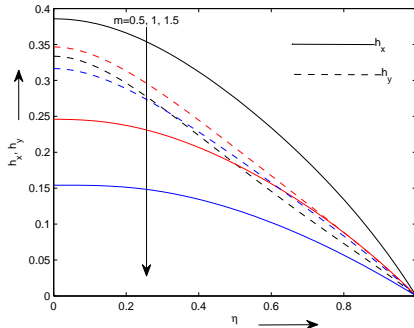


Figure 6: Induced magnetic field profiles when  $K^2 = 7$ ,  $M^2 = 10$  and  $K_1 = 0.2$ .

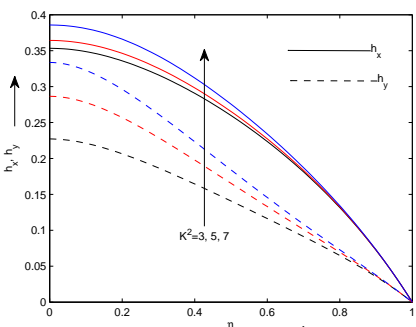


Figure 7: Induced magnetic field profiles when  $m = 0.5$ ,  $M^2 = 10$  and  $K_1 = 0.2$ .

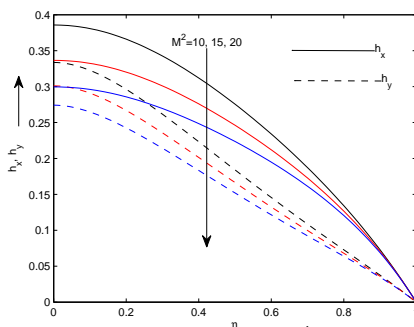


Figure 8: Induced magnetic field profiles when  $m = 0.5$ ,  $K^2 = 7$  and  $K_1 = 0.2$ .

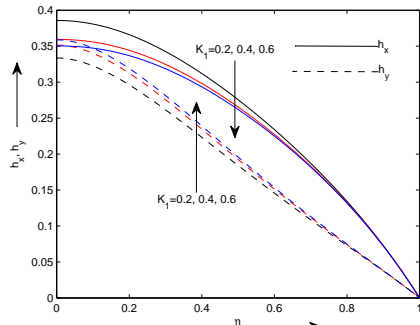


Figure 9: Induced magnetic field profiles when  $m = 0.5$ ,  $K^2 = 7$  and  $M^2 = 10$ .

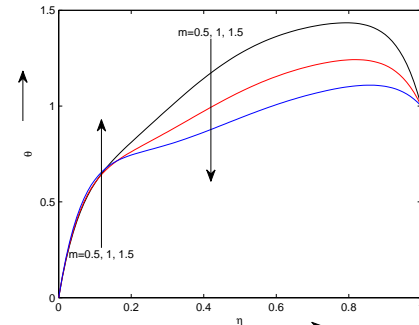


Figure 10: Temperature profiles when  $K^2 = 7$ ,  $M^2 = 10$  and  $K_1 = 0.2$ .

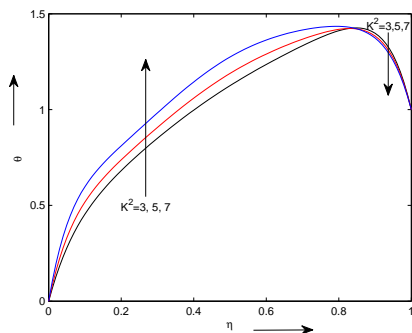


Figure 11: Temperature profiles when  $m = 0.5$ ,  $M^2 = 10$  and  $K_1 = 0.2$ .

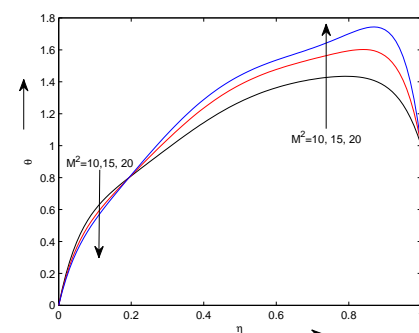


Figure 12: Temperature profiles when  $m = 0.5$ ,  $K^2 = 7$  and  $K_1 = 0.2$ .

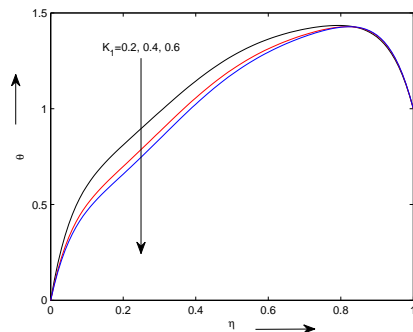


Figure 13: Temperature profiles when  $m = 0.5$ ,  $K^2 = 7$  and  $M^2 = 10$ .

Table 2: Shear stress at the stationary plate when  $M^2 = 10$  and  $K_1 = 0.2$ .

$K^2 \downarrow m \rightarrow$	$\tau_x  _{\eta=0}$			$\tau_y  _{\eta=0}$		
	0.5	1	1.5	0.5	1	1.5
3	1.6824	1.8524	2.0026	0.9156	0.7967	0.7596
5	1.9523	2.1359	2.2885	1.5654	1.4435	1.4078
7	2.2646	2.4523	2.6044	2.1151	1.9824	1.9426

Table 3: Shear stress at the stationary plate when  $m = 0.5$  and  $K^2 = 7$ .

$K_1 \downarrow M^2 \rightarrow$	$\tau_x  _{\eta=0}$			$\tau_y  _{\eta=0}$		
	10	15	20	10	15	20
0.2	2.2646	2.0061	1.8111	2.1151	2.0281	1.9423
0.4	1.9489	1.6860	1.4928	2.3336	2.2314	2.1298
0.6	1.8439	1.5787	1.3857	2.4148	2.3065	2.1986

Table 4: Shear stress at the moving plate when  $M^2 = 10$  and  $K_1 = 0.2$ .

$K^2 \downarrow m \rightarrow$	$\tau_x  _{\eta=1}$			$\tau_y  _{\eta=1}$		
	0.5	1	1.5	0.5	1	1.5
3	2.2472	1.7616	1.3699	0.2405	0.5540	0.6050
5	2.0884	1.6151	1.2316	0.0269	0.3611	0.4299
7	1.9148	1.4644	1.0947	-0.1098	0.2468	0.3353

Table 5: Shear stress at the moving plate when  $m = 0.5$  and  $K^2 = 7$ .

$K_1 \downarrow M^2 \rightarrow$	$\tau_x  _{\eta=1}$			$\tau_y  _{\eta=1}$		
	10	15	20	10	15	20
0.2	1.9148	2.6291	3.2454	-0.1098	0.0261	0.1595
0.4	1.9761	2.7150	3.3460	-0.2288	-0.0876	0.0536
0.6	1.9943	2.7427	3.3793	-0.2744	-0.1308	0.0137

Table 6: Mass flow rates when  $M^2 = 10$  and  $K_1 = 0.2$ .

$K^2 \downarrow m \rightarrow$	$Q_x$			$Q_y$		
	0.5	1	1.5	0.5	1	1.5
3	0.4669	0.5087	0.5470	0.0505	0.0162	0.0048
5	0.5075	0.5494	0.5871	0.1044	0.0677	0.0547
7	0.5525	0.5925	0.6287	0.1407	0.1007	0.0853

Table 7: Mass flow rates when  $m = 0.5$  and  $K^2 = 7$ .

$K_1 \downarrow M^2 \rightarrow$	$Q_x$			$Q_y$		
	10	15	20	10	15	20
0.2	0.5525	0.4870	0.4366	0.1407	0.1328	0.1243
0.4	0.5352	0.4667	0.4150	0.1718	0.1619	0.1511
0.6	0.5298	0.4600	0.4077	0.1836	0.1728	0.1610

Table 8: Rate of heat transfer at stationary and moving plates when  $M^2 = 10$ ,  $K_1 = 0.2$ ,  $P_r = 7$  and  $E_c = 0.2$ .

$K^2 \downarrow m \rightarrow$	$\frac{d\theta}{d\eta}  _{\eta=0}$			$-\frac{d\theta}{d\eta}  _{\eta=1}$		
	0.5	1	1.5	0.5	1	1.5
3	7.0683	7.3462	7.7112	8.1756	4.8871	2.7237
5	8.8834	9.1520	9.5534	7.6536	4.4172	2.3451
7	11.2213	11.4606	11.8897	7.1751	4.0438	2.0714

Table 9: Rate of heat transfer at stationary and moving plates when  $m = 0.5$ ,  $K^2 = 7$ ,  $P_r = 7$  and  $E_c = 0.2$ .

$K_1 \downarrow M^2 \rightarrow$	$\frac{d\theta}{d\eta}  _{\eta=0}$			$-\frac{d\theta}{d\eta}  _{\eta=1}$		
	10	15	20	10	15	20
0.2	11.2213	10.1963	9.4369	7.1751	12.2390	17.5908
0.4	9.2205	8.2253	7.4852	7.3701	12.5653	18.0389
0.6	8.6287	7.6353	6.8942	7.4367	12.6778	18.1941

Table 10: Rate of heat transfer at stationary and moving plates when  $m = 0.5$ ,  $K^2 = 7$ ,  $M^2 = 10$  and  $K_1 = 0.2$ .

$P_r \downarrow E_c \rightarrow$	$\frac{d\theta}{d\eta}  _{\eta=0}$			$-\frac{d\theta}{d\eta}  _{\eta=1}$		
	0.2	0.4	0.6	0.2	0.4	0.6
1	2.4602	3.9204	5.3806	0.1679	1.3357	2.5036
3	5.3806	9.7611	14.1417	2.5036	6.0072	9.5108
7	11.2213	21.4426	31.6639	7.1751	15.3501	23.5252

## 7 Conclusions

In this paper investigation on steady hydromagnetic Couette flow of class-II and heat transfer of a viscous, incompressible and electrically conducting

fluid through a uniform porous medium in a rotating system taking Hall current into account is carried out. The significant results are summarized below:

- It is found that there arises a thin modified Ekman boundary layer for large values of  $K^2$  and a thin modified Hartmann boundary layer for large values of  $M^2$  near the plates of the channel.
- Hall current tends to accelerate fluid flow in the primary flow direction whereas it has a reverse effect on the fluid flow in the secondary flow direction. Rotation tends to accelerate fluid flow in both the primary and secondary flow directions whereas magnetic field has a reverse effect on it. Permeability of the medium tends to decelerate fluid flow in the primary flow direction whereas it has a reverse effect on the fluid flow in the secondary flow direction.
- Hall current tends to reduce primary induced magnetic field. Rotation tends to enhance both the primary and secondary induced magnetic fields whereas magnetic field has a reverse effect on it. Permeability of the medium tends to reduce primary induced magnetic field whereas it has a reverse effect on the secondary induced magnetic field.
- There exists flow separation at the moving plate in the secondary flow direction on increasing either  $K^2$  when  $m = 0.5$  or  $m$  when  $K^2 = 7$ . Also there exists flow separation at the moving plate in the secondary flow direction on increasing either  $M^2$  for every value of  $K_1$  or  $K_1$  when  $M^2 = 15$ .
- In most of the region of the channel, Hall current tends to reduce fluid temperature whereas rotation and magnetic field have reverse effect on it. Permeability of the medium tends to reduce fluid temperature throughout the channel.
- Hall current and rotation tend to enhance rate of heat transfer at the stationary plate whereas these agencies have reverse effect on the rate of heat transfer at the moving plate. Magnetic field and permeability of the medium tend to reduce rate of heat transfer at the stationary plate whereas these agencies have reverse effect on the rate of heat transfer at the moving plate. Thermal diffusion tends to reduce rate of heat transfer at both the plates whereas viscous dissipation has a reverse effect on it.

## References

- [1] S. Ahmed and A. J. Chamkha, *Hartmann Newtonian radiating MHD flow for a rotating vertical porous channel immersed in a Darcian porous regime: An exact solution*, Int. J. Numerical Methods for Heat Fluid Flow **24** (2014) 1454-1470.
- [2] S. Ahmed and K. Kalita, *A sinusoidal fluid injection/suction on MHD three dimensional Couette flow through a porous medium in the presence of thermal radiation*, J. Energy, Heat Mass Transfer **35** (2013) 41-67.
- [3] S. Ahmed and K. Kalita, *Magnetohydrodynamic transient flow through a porous medium bounded by a hot vertical plate in presence of radiation: A theoretical analysis*, J. Eng. Phys. Thermophys. **86** (2013) 31-39.
- [4] S. Ahmed and K. Kalita, *Unsteady MHD chemical reacting fluid through a porous medium bounded by a non-isothermal impulsively-started vertical plate: A numerical technique*, J. Naval Architecture Marine Eng. **11** (2014) 39-54.
- [5] S. Ahmed, *Numerical analysis for magnetohydrodynamic chemically reacting and radiating fluid past a non-isothermal impulsively started vertical surface adjacent to a porous regime*, Ain Shams Eng. J. **5** (2014) 923-933.
- [6] S. Ahmed and J. Zueco, *Modelling of heat and mass transfer in a rotating vertical channel with Hall current*, Chem. Eng. Communications, **198** (2011) 1294-1308.
- [7] K. D. Alagoa, G. Tay and T. M. Abbey, *Radiative and free convective effects of a MHD flow through a porous medium between infinite parallel plates with time-dependent suction*, Astrophys. Space Sci. **260** (1999) 455-468.
- [8] G. K. Batchelor, *An introduction to fluid dynamics*, Cambridge Univ. Press, Cambridge (U.K.), 1988.
- [9] K. Chand, K. D. Singh and S. Kumar, *Oscillatory free convective flow of viscoelastic fluid through porous medium in a rotating vertical channel*, Proc. Natl. Acad. Sci., India, Sect. A Phys. Sci. **83** (2013) 333-342.
- [10] R. K. Cramer and S. I. Pai, *Magnetofluid dynamics for engineers and applied physicists*, McGraw-Hill Book Company, New York, 1973.

- [11] A. J. Chamkha, *A note on unsteady hydromagnetic free convection from a vertical fluid saturated porous medium channel*, ASME J. Heat Transfer **119** (1997) 638-641.
- [12] A. J. Chamkha, *Flow of two-immiscible fluids in porous and non-porous channels*, ASME J. Fluid Eng. **122** (2000) 117-124.
- [13] A. J. Chamkha, *Non-Darcy fully developed mixed convection in a porous medium channel with heat generation/absorption and hydromagnetic effects*, Numerical Heat transfer, Part A **32** (1997) 653-675.
- [14] A. J. Chamkha, *Unsteady laminar hydromagnetic flow and heat transfer in porous channels with temperature-dependent properties*, Int. J. Numerical Methods for Heat Fluid Flow **11** (2001) 430-448.
- [15] B. K. Das, M. Guria and R. N. Jana, *Unsteady Couette flow in a rotating system*, Meccanica **43** (2008) 517-521.
- [16] S. Das, B. C. Sarkar and R. N. Jana, *Hall effects on hydromagnetic rotating Couette flow*, Int. J. Comp. Applications **83** (2013) 20-26.
- [17] S. Das, B. C. Sarkar and R. N. Jana, *Hall effects on MHD Couette flow in rotating system*, Int. J. Comp. Applications **35** (2011) 22-30.
- [18] R. Ganapathy, *A note on oscillatory Couette flow in a rotating system*, Trans. ASME J. Appl. Mech. **61** (1994) 208-209.
- [19] T. Hayat, S. Nadeem and S. Asghar, *Hydromagnetic Couette flow of an oldroyd-B fluid in a rotating system*, Int. J. Eng. Sci. **42** (2004) 65-78.
- [20] T. Hayat, S. Nadeem, A. M. Siddiqui and S. Asghar, *An oscillatory hydromagnetic non-Newtonian flow in a rotating system*, Appl. Math. Lett. **17** (2004) 609-614.
- [21] C. Israel-Cooke, E. Amos and C. Nwaigwe, *MHD oscillatory Couette flow of a radiating viscous fluid in a porous medium with periodic wall temperature*, Am. J. Sci. Ind. Res. **1** (2010) 326-331.
- [22] R. N. Jana and N. Datta, *Hall effects on MHD Couette flow in a rotating system*, Czech. J. Phys. B **30** (1980) 659-667.
- [23] R. N. Jana, N. Datta and B. S. Mazumder, *Magnetohydrodynamic Couette flow and heat transfer in a rotating system*, J. Phys. Soc. Jpn. **42** (1977) 1034-1039.

- [24] M. Jana, S. Das and R. N. Jana, *Unsteady Couette flow through a porous medium in a rotating system*, Open J. Fluid Dynamics **2** (2012) 149-158.
- [25] O. D. Makinde and P. Y. Mhone, *Heat transfer to MHD oscillatory flow in a channel filled with porous medium*, Rom. J. Phys. **50** (2005) 931-938.
- [26] G. Mandal, K. K. Mandal and G. Choudhury, *On combined effects of Coriolis force and Hall current on steady MHD Couette flow and heat transfer*, J. Phys. Soc. Jpn. **51** (1982) 2010-2015.
- [27] B. S. Mazumder, *An exact solution of oscillatory Couette flow in a rotating system*, Trans. ASME J. Appl. Mech. **58** (1991) 1104-1107.
- [28] B. G. Prasad and R. Kumar, *Unsteady hydromagnetic Couette flow through a porous medium in a rotating system*, Theor. Appl. Mech. Lett. **1** (2011) 042005.
- [29] B. C. Sarkar, S. Das and R. N. Jana, *Combined effects of Hall currents and rotation on steady hydromagnetic Couette flow*, Res. J. Appl. Sci. Eng. Tech. **5** (2013) 1864-1875.
- [30] G. S. Seth and N. Ahmad, *Effects of Hall current on MHD Couette flow and heat transfer in a rotating system*, J. ISTM **30** (1985) 177-188.
- [31] G. S. Seth, G. K. Mahato and J. K. Singh, *Effects of Hall current and rotation on MHD Couette flow of class-II*, J. Int. Acad. Phys. Sci. **15** (2011) 201-219.
- [32] G. S. Seth, R. Sharma, P. Kumari and S. Sarkar, *Effects of Hall current and rotation on MHD Couette flow of class-II in the presence of an inclined magnetic field*, J. Nature Sci. Sustainable Tech. **8** (2014) 27-50.
- [33] G. S. Seth and S. M. Hussain, *Hall effects on hydromagnetic Couette flow of class-II in a rotating system in the presence of an inclined magnetic field with asymmetric heating/cooling of the walls*, Int. J. Eng. Sci. Tech. **3** (2011) 234-247.
- [34] G. S. Seth and M. K. Maiti, *MHD Couette flow and heat transfer in a rotating system*, Ind. J. Pure Appl. Math. **13** (1982) 931-945.

- [35] G. S. Seth, S. M. Hussain and J. K. Singh, *MHD Couette flow of class-II in a rotating system*, J. Appl. Math. Bioinformatics **1** (2011) 31-54.
- [36] G. S. Seth and J. K. Singh, *Steady hydromagnetic Couette flow in a rotating system with non-conducting walls*, Int. J. Eng. Sci. Tech. **3** (2011) 146-156.
- [37] G. S. Seth and J. K. Singh, *Unsteady MHD Couette flow of class-II of a viscous incompressible electrically conducting fluid in a rotating system*, Int. J. Appl. Mech. Eng. **17** (2012) 495-512.
- [38] G. S. Seth, R. Nandkeolyar and M. S. Ansari, *Hall effects on oscillatory hydromagnetic Couette flow in a rotating system*, Int. J. Acad. Res. **1** (2009) 6-17.
- [39] G. S. Seth and J. K. Singh, *Effects of Hall current on unsteady MHD Couette flow of class-II in a rotating system*, J. Appl. Fluid Mech. **6** (2013) 473-484.
- [40] K. D. Singh, *An oscillatory hydromagnetic Couette flow in a rotating system*, J. Appl. Math. Mech. **80** (2000) 429-432.
- [41] K. D. Singh, *Effect of injection/suction on convective oscillatory flow through porous medium bounded by two vertical porous plates*, Int. J. Phys. Math. Sci. **2** (2011) 140-147.
- [42] K. D. Singh, *Exact solution of an oscillatory MHD flow on a channel filled with porous medium*, Int. J. Appl. Mech. Eng. **16** (2011) 277-283.
- [43] K. D. Singh, M. G. Gorla and Hansraj, *A periodic solution of oscillatory Couette flow through a porous medium in rotating system*, Ind. J. Pure Appl. Math. **36** (2005) 151-159.
- [44] K. D. Singh and A. Mathew, *An oscillatory free convective flow through porous medium in a rotating vertical porous channel*, Global J. Sci. Front. Res. **12** (2012) 51-64.
- [45] G. W. Sutton and A. Sherman, *Engineering Magnetohydrodynamics*, McGraw-Hill, 1965.
- [46] J. C. Umarathai, J. P. Kumar, A. J. Chamkha and I. Pop, *Mixed convection in a vertical porous channel*, Transport in Porous Media **61** (2005) 315-335.

- [47] J. C. Umapathi, A. J. Chamkha and K. S. R. Sridhar, *Generalized plain Couette flow and heat transfer in a composite channel*, Transport in Porous Media **85** (2010) 157-169.

